Inorg. Chem. **2007**, *46*, 3876–3888

Binding of Nitrate to a Cu^{II}–Cyclen Complex Bearing a Ferrocenyl Pendant: Synthesis, Solid-State X-ray Structure, and Solution-Phase Electrochemical and Spectrophotometric Studies

Gilles Gasser, Matthew J. Belousoff, Alan M. Bond, and Leone Spiccia*

School of Chemistry, Monash University, Clayton, Victoria 3800, Australia

Received August 29, 2006

The reaction of $Cu(NO_3)_2 \cdot 3H_2O$ with the ligand 1-(ferrocenemethyl)-1,4,7,10-tetraazacyclododecane (**L**) in acetonitrile leads to the formation of a blue complex, $[Cu(\mathbf{L})(NO_3)][NO_3]$ (**C1**). The X-ray structure determination shows an unexpected binding of a nitrate anion in that the Cu^{II} center is surrounded by four N atoms of the 1,4,7,10-tetraazacyclododecane (cyclen) macrocycle and two O atoms from a chelating nitrate anion, both Cu–O distances being below the sums of the van de Waals radii. Hydrogen-bonding interactions in the crystal lattice and a weak interaction between a second nitrate O and the Cu^{II} center in **C1** give rise to a highly distorted Cu^{II} geometry relative to that found in the known structure of $[Cu(cyclen)(NO_3)][NO_3]$ (**C5**). Electrochemical studies in acetonitrile containing 0.1 M $[Bu_4N][NO_3]$ as the supporting electrolyte showed that oxidation of **C1** in this medium exhibits a single reversible one-electron step with a formal potential $E°_f$ of +85 mV vs $Fc^{0/+}$ (Fc = ferrocene). This process is associated with oxidation of the ferrocenyl pendant group. Additionally, a reversible one-electron reduction reaction with an $E°_f$ value of –932 mV vs $Fc^{0/+}$, attributed to the $Cu^{II/I}$ redox couple, is detected. Gradual change of the supporting electrolyte from 0.1 M $[Bu_4N][NO_3]$ to the poorly coordinating $[Bu_4N][PF_6]$ electrolyte, at constant ionic strength, led to a positive potential shift in $E°_f$ values by +107 and +39 mV for the $Cu^{II/I}$**(C1)** and $Fc^{0/+}$(**C1**) redox couples, respectively. Analysis of these electrochemical data and UV–vis spectra is consistent with the probable presence of the complexes **C1**, $[Cu(\mathbf{L})(CH_3CN)_2]^{2+}$ (**C2**), $[Cu(\mathbf{L})(CH_3CN)(NO_3)]^{+}$ (**C3**), and $[Cu(\mathbf{L})(NO_3)_2]$ (**C4**) as the major species in nitrate-containing acetonitrile solutions. In weakly solvating nitromethane, the extent of nitrate complexation remains significant even at low nitrate concentrations, due to the lack of solvent competition.

Introduction

Metal complexes of the 1,4,7,10-tetraazacyclododecane (cyclen) macrocycle and its derivatives have been used in a wide range of medical applications, which include contrast-enhancing agents in magnetic resonance imaging,[1] radiotherapy,[2] models for protein−metal binding sites in biological systems,[3] and RNA cleavage catalysts.[4] In the sensing area, Aoki and Kimura showed that the Zn^{II}−cyclen complex selectively binds thymine derivatives in aqueous solution at physiological pH levels.[5] As a consequence, the development of potentially specific redox biosensors for DNA bases could be envisioned when anthraquinone[6] or ferrocene moieties[7,8] were covalently attached to the Zn^{II}−cyclen complex to act as the redox signaling units. Voltammetric oxidation of the ferrocene center has been widely used for sensing purposes,[9−14]

* To whom correspondence should be addressed. E-mail: leone.spiccia@sci.monash.edu.au. Fax: +61 3 9905 4597.

(1) Zhang, S.; Jiang, X.; Sherry, A. D. *Helv. Chim. Acta* **2005**, *88*, 923−935 and references therein.
(2) Reichert, D. E.; Lewis, J.; Anderson, C. J. *Coord. Chem. Rev.* **1999**, *184*, 3−66 and references therein.
(3) Kimura, E. *Pure Appl. Chem.* **1993**, *65*, 355.
(4) Epstein, D. M.; Chappell, L. L.; Khalili, H.; Supkowski, R. M.; Horrocks, W. D., Jr.; Morrow, J. R. *Inorg. Chem.* **2000**, 39, 2130−2134 and references therein.
(5) Aoki, S.; Kimura, E. *Chem. Rev.* **2004**, 104, 769−787 and references therein.
(6) Tucker, J. H. R.; Shionoya, M.; Koike, T.; Kimura, E. *Bull. Chem. Soc. Jpn.* **1995**, *68*, 2465−2469.
(7) Gasser, G.; Bond, A. M.; Graham, B.; Kosowski, Z.; Spiccia, L. *NSTI Nanotech 2005*; Proceedings of the NSTI Nanotechnology Conference and Trade Show, Anaheim, CA, May 8−12, 2005; Nano Science and Technology Institute: Cambridge, MA, 2005; pp 412−415.
(8) Gasser, G.; Belousoff, M. J.; Bond, A. M.; Kosowski, Z.; Spiccia, L. *Inorg. Chem.* **2007**,, *46*, 1665−1674.
(9) Plenio, H.; Aberle, C.; Shihadeh, Y. A.; Lloris, J. M.; Martinez-Manez, R.; Pardo, T.; Soto, J. *Chem.—Eur. J.* **2001**, *7*(13), 2848−2861 and references therein.
(10) van Stavaren, D. R.; Metzler-Nolte, N. *Chem. Rev.* **2004**, *104*, 5931−5985 and references therein.

10.1021/ic061622+ CCC: $37.00
Published on Web 04/17/2007

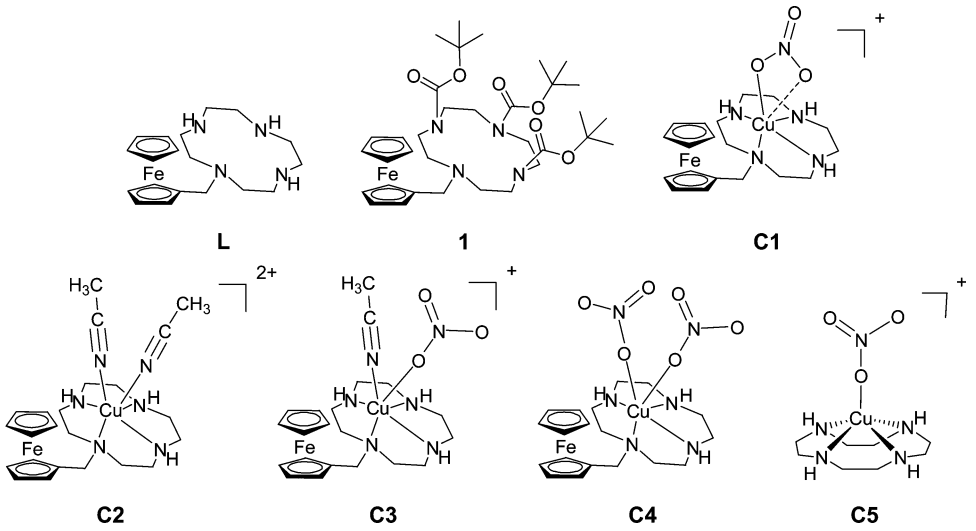

Figure 1. Representations of the structures of **L**, **1**, **C1** (solid state), and **C5** (solid state) and **C2**−**C4**.

due to its well-defined reversible behavior. Macrocyles bearing a ferrocenyl unit have also been applied in the selective electrochemical recognition of anions, such as dihydrogenphosphate, chloride, hydrogensulfate, or acetate. Generally, this is achieved through hydrogen bonding, electrostatic interaction, or coordination to a metal cation, with anion complexation in close proximity to the redox-active fragment to allow electrochemical detection of the guest.[15] Recently, Saint-Aman and co-workers described a ferrocenyl receptor that combined two of these binding modes.[16]

To enhance the electrochemical sensing response of anions, Beer and co-workers synthesized receptors that contain two different redox-active moieties so that dihydrogenphosphate, chloride, bromide, hydrogensulfate, nitrate, or acetate binding could be monitored by more than one electrochemical response. Examples of their strategy include ferrocene and an additional electrochemically active Lewis acid transition-metal center,[17] dithiocarbamate−copper(II) complexes that contain two copper ions and exhibit well-separated reversible oxidation waves,[18] ferrocene and metalloporphyrins,[19] and ruthenium complexes combined with ferrocene, cobaltocene, or an osmium complex.[20] However, in all these studies, anion binding does not involve direct coordination to a metal center. With this concept of using two redox-active centers in mind, we have been investigating the coordination chemistry of the ligand 1-(ferrocenemethyl)-1,4,7,10-tetraazacyclododecane (**L**) (see Figure 1) and the ability of the resulting complex to act as an anion recognition agent. This led to the synthesis and X-ray structure of a novel Cu(II) complex of **L**, $[Cu\mathbf{L}(NO_3)]^+$ (**C1**) (see Figure 1), in which the nitrate anion adopts an orientation that significantly distorts the copper coordination sphere. Electrochemical studies in acetonitrile and nitromethane as a function of nitrate concentration demonstrate that recognition of the nitrate ion occurs with respect to both the $Fc^{0/+}$ (Fc = ferrocene) and the $Cu^{II/I}$ redox couples. These data in conjunction with spectrophotometric measurements allow the species present in solution to be probed and compared to those found in the solid state.

Experimental Section

Materials. All chemicals were of reagent-grade purity or better and were used as obtained from the commercial suppliers. High-purity nitrogen gas was used to degas solutions used in electrochemical experiments. Deionized water was distilled prior to use.

Instrumentation. ^{1}H and ^{13}C NMR spectra were recorded in deuterated solvents on Bruker AC200, Bruker DPX300, or Avance DRX400 Bruker spectrometers at 30 °C. The chemical shifts, δ, are reported in ppm. Tetramethylsilane or the residual solvent peaks were used as internal references. The abbreviations for the peak multiplicities are as follows: s (singlet), d (doublet), dd (doublet of doublets), t (triplet), q (quartet), m (multiplet), and br (broad). Infrared spectra using KBr disks were recorded with a Bruker IFS 55 FTIR spectrophotometer at a resolution of 4 cm^{-1}. UV−vis spectra were recorded in 1 cm quartz cuvettes using either a Varian Cary 300 or a Varian Cary 5G spectrophotometer. All solutions were filtered with nylon filters (0.45 μm) before being analyzed. To fully dissolve the complex, solutions sometimes needed to be warmed in a water bath. Low-resolution electrospray ionization mass spectra (ESIMS) were obtained with a Micromass Platform II Quadrupole mass spectrometer fitted with an electrospray source. High-resolution MS data were recorded on a Bruker BioApex II 47e FT-ICR MS fitted with an Analytica Electrospray Source. Samples were introduced by a syringe pump at a flow rate of 1 μL min^{-1}. The capillary voltage was 200 V. CHN analyses were performed by the Campbell Microanalytical Services, University of Otago, Dunedin, New Zealand.

(11) Kraatz, H.-B. *J. Inorg. Organomet. Polym. Mater.* **2005**, *15* (1), 83−106 and references therein.
(12) Plenio, H.; Aberle, C. *Angew. Chem., Int. Ed.* **1998**, *37* (10), 1397−1399 and references therein.
(13) Takaneka, S. *Polym. J.* **2004**, *36* (7), 503−512 and references therein.
(14) Tucker, J. H. R.; Collinson, S. R. *Chem. Soc. Rev.* **2002**, *31*, 147−156 and reference therein.
(15) Schmidtchen, F. P.; Berger, M. *Chem. Rev.* **1997**, *97*, 1609−1646 and references therein.
(16) Bucher, C.; Devillers, C. H.; Moutet, J.-C.; Royal, G.; Saint-Aman, E. *New J. Chem.* **2004**, *12*, 1584−1589.
(17) Kingston, J. E.; Ashford, L.; Beer, P. D.; Drew, M. G. B. *J. Chem. Soc., Dalton Trans.* **1999**, 251−257.
(18) Beer, P. D.; Berry, N.; Drew, M. G. B.; Danny Fox, O.; Padilla-Tosta, M. E.; Patell, S. *Chem. Commun.* **2001**, 199−200.
(19) Beer, P. D. *Chem. Commun.* **1996**, 689.
(20) Beer, P. D.; Szemes, F.; Balzani, V.; Salà, C. M.; Drew, M. G. B.; Dent, S. W.; Maestri, M. *J. Am. Chem. Soc.* **1997**, *119*, 11864.

Electrochemical Studies. All voltammetric measurements were performed with a BAS Epsilon potentiostat operated by BASi Epsilon-EC Software, version 1.50.69_XP. A typical three-electrode cell was employed, comprising a Pt counter electrode, an $Ag/AgNO_3$ (acetonitrile, 10 mM $AgNO_3$) reference electrode, and a 3.06 mm diameter glassy-carbon (GC) working electrode. To avoid overlap with the oxidation of the ferrocenyl pendant group, the voltammetrically reversible one-electron decamethylferrocene couple ($Cp^*_2Fe^{0/+}$; Cp* = pentamethylcyclopentadienyl) was used as a secondary internal reference (0.25 mM). Standard potentials were then referenced to the usual $Fc^{0/+}$ couple using measured values for the $Cp^*_2Fe^{0/+}$ process (−505 mV vs $Fc^{0/+}$ in acetonitrile and −508 mV vs $Fc^{0/+}$ in nitromethane as determined in the presence of Bu_4NPF_6 (0.1 M) as the supporting electrolyte and with a scan rate of 100 mV s^{-1}). It was assumed that these potential conversion values are independent of the electrolyte and scan rate. The voltammetry for oxidation of Fc was used to calculate the area of the GC working electrode (0.07 cm^2) by using the Randles-Sevcik equation and a diffusion coefficient of Fc of 1.70×10^{-5} cm^2 s^{-1} in acetonitrile (0.5 M $[Bu_4N][PF_6]$).[21,22] All measurements were recorded over a scan-rate range of 10−1000 mV s^{-1} at (20 ± 2) °C inside a Faraday cage under a N_2 atmosphere to minimize electrochemical noise and atmospheric O_2/H_2O interference, respectively.

Synthesis. 1-(Ferrocenemethyl)-1,4,7,10-tetraazacyclododecane (L). L was synthesized following the general procedure published by Sisti et al. and involved a three-step reaction sequence starting from commercially available cyclen.[23] However, the following two improvements were introduced. After a first step to obtain the triprotected cyclen compound, 1,4,7-triformyl-1,4,7,10-tetraazacyclododecane, the second step involving the synthesis of 1-(ferrocenemethyl)-4,7,10-triformyl-1,4,7,10-tetraazacyclododecane was performed by refluxing the reagents used in Sisti's procedure (without base) for 16 h in deoxygenated water instead of DMF. Purification was carried out by chromatography on a silica column with CH_2Cl_2/MeOH in a 20:1 ratio as the eluent (R_f = 0.45). An increase in the yield from 53 to 65% was obtained via this modified procedure. The deprotection of the formyl groups was then carried out by heating, for 24 h, 1-(ferrocenemethyl)-4,7,10-triformyl-1,4,7,10-tetraazacyclododecane at 80 °C in 1 M NaOH instead of 0.2 M NaOH. Purification of the final product **L** was performed by chromatography on a silica column with MeOH/diethylamine in a 10:1 ratio as the eluent (R_f = 0.31). The required compound obtained after chromatography was dissolved in a minimal amount of CH_2Cl_2 and filtered to remove any silica that might have dissolved in the eluent. The filtered organic phase was then washed with water to remove any inorganic salts that were present. Anal. Calcd for $FeC_{19}H_{30}N_4 \cdot H_2O$: C, 58.8; H, 8.3; N, 14.4. Found: C, 59.3; H, 7.8; N, 14.0. Major IR bands (KBr; ν, cm^{-1}): 3422 m br, 3205 m, 3091 m, 2928 s, 2818 s, 1719 w, 1655 m, 1561 m, 1545 m, 1458 s, 1330 m, 1223 m, 1104 s, 1038 s, 925 m, 803 s, 736 m. UV−vis ($CHCl_3$, λ (nm), ϵ (M^{-1} cm^{-1})): 433, 134. ^{1}H NMR ($CDCl_3$): δ 2.48−2.63 (m, 13H, CH_2 cyclen ring and N*H*), 2.75−2.82 (m, 5H, CH_2 cyclen and N*H*), 3.49 (s, 1H, N*H*), 3.56 (s, 2H, Cp−CH_2−cyclen), 4.08−4.12 (m, 9H, C*H* Cp ring). ^{13}C NMR ($CDCl_3$): δ 45.32 (*C*H_2 cyclen), 46.40 (*C*H_2 cyclen), 47.38 (*C*H_2 cyclen), 50.68 (*C*H_2 cyclen), 54.05 (Cp−*C*H_2−cyclen), 68.15 (*C*H Cp), 68.63 (*C*H Cp), 70.24 (*C*H Cp), 83.01 (*C* Cp). ESIMS (*m*/*z*): 199 $[Fc-CH_2]^+$ (32%), 371 $[M + H]^+$ (100%).

1,4,7-Tris-*tert*-butoxycarbonyl-1,4,7,10-tetraazacyclododecane. This compound was synthesized following the procedure of Wieghardt et al.[24] The analytical data matched that reported previously.[24]

(Ferrocenylmethyl)trimethylammonium Iodide. This compound was synthesized following the procedure of Lindsay and Hauser.[25] The analytical data of the product matched that reported previously.[25]

1,4,7-Tris-*tert*-butoxycarbonyl-10-(ferrocenylmethyl)-1,4,7,-10-tetraazacyclododecane (1). 1,4,7-Tris-*tert*-butoxycarbonyl-1,4,7,10-tetraazacyclododecane (0.75 g, 1.58 mmol), (ferrocenylmethyl)trimethylammonium iodide (0.61 g, 1.58 mmol), and K_2CO_3 (1.09 g, 7.90 mmol) were refluxed in anhydrous DMF (20 mL) for 18 h. The solvent was then removed under reduced pressure, and CH_2Cl_2 (25 mL) was poured onto the black-brown residue. The suspended solid was removed by filtration, and the filtrate was washed with water (3 × 15 mL). The solvent in the organic phase was removed under reduced pressure to give an orange sticky-solid residue. Purification by chromatography on a silica column was performed with CH_2Cl_2/acetone in a 25:1 ratio as the eluent (R_f = 0.30). The desired fractions were evaporated to dryness to yield **1** as an orange solid. Yield: 0.45 g (42%). Anal. Calcd for $FeC_{34}H_{54}N_4O_6 \cdot {}^1/_2CH_2Cl_2$: C, 58.1; H, 7.8; N, 7.9. Found: C, 58.5; H, 7.9; N, 7.9. Major IR bands (KBr; ν, cm^{-1}): 3095 w, 2976 m, 1686 s, 1559 m, 1415 s, 1362 s, 1316 w, 1250 s, 1172 s, 1104 m, 1025 w, 979 w, 920 w, 884 w, 859 w, 820 w, 772 w, 733 w, 645 w. ^{1}H NMR ($CDCl_3$): δ 1.43 (s, 18H, O−C(CH_3)$_3$), 1.46 (s, 9H, O−C(CH_3)$_3$), 2.48−2.63 (m, 4H, CH_2 cyclen ring), 3.15−3.58 (m, 14H, CH_2 cyclen ring and Cp−CH_2−cyclen), 4.05−4.15 (m, 9H, C*H* Cp ring). ^{13}C NMR ($CDCl_3$): δ 28.70 (O−C(*C*H_3)$_3$), 28.90 (O−C(*C*H_3)$_3$), 47.38 (*C*H_2 cyclen), 47.76 (*C*H_2 cyclen), 48.24 (*C*H_2 cyclen), 54.24 (*C*H_2 cyclen), 55.75 (Cp−*C*H_2−cyclen), 68.44 (*C*H Cp), 68.73 (*C*H Cp), 70.69 (*C*H Cp), 79.37 (*C* Cp), 79.56 (O−*C*(CH$_3$)$_3$), 79.65 (O−*C*(CH$_3$)$_3$), 155.58 (N−*C*OO), 155.84 (N−*C*OO). ESIMS (*m*/*z*): 671 $[M + H]^+$ (100%). High-resolution ESI mass determination: found, 671.3464; calcd for $FeC_{34}H_{55}N_4O_6$, 671.3471.

[Cu(L)(NO$_3$)][NO$_3$] (C1). L (50 mg, 0.14 mmol) and $Cu(NO_3)_2 \cdot 3H_2O$ (32 mg, 0.14 mmol) were dissolved in ethanol (15 mL) and refluxed for 30 min. After cooling to room temperature, diethyl ether was added to precipitate the complex, which was filtered, washed with diethyl ether, and dried. Blue crystals suitable for X-ray crystallography were obtained by diffusion of diethyl ether into an acetonitrile solution of **C1**. Yield: 61 mg (81%). Anal. Calcd for $CuFeC_{19}H_{30}N_6O_6$: C, 40.9; H, 5.4; N, 15.1. Found: C, 40.8; H, 5.3; N, 14.8. Major IR bands (KBr; ν, cm^{-1}): 3179 s br, 2918 s, 1633 m, 1382 vs, 1234 m, 1104 s, 1081 s, 999 m, 815 m, 742 w, 592 w, 513 w. ESIMS (*m*/*z*): 199 $[Fc-CH_2]^+$ (38%), 432 $[L + Cu - H]^+$ (100%), 495 $[\mathbf{C1}]^+$ (15%).

Nitrato(1,4,7,10-tetraazacyclododecane)copper(II) Nitrate (C5). **C5** was synthesized following the procedure described by Styka et al.[26] Blue crystals suitable for X-ray crystallography were obtained by diffusion of diethyl ether into a solution of **C5** in acetonitrile. The unit cell was the same as that reported in the literature.[27] Major IR bands (KBr; ν, cm^{-1}): 3171 m br, 2927 m, 1629 w, 1382 s,

(21) Bard, A. J.; Faulkner, L. R. *Electrochemical Methods—Fundamentals and Applications*; Wiley: New York, 2002.
(22) Mirkin, M. V.; Richards, T. C.; Bard, A. J. *J. Phys. Chem.* **1993**, *97*, 7671.
(23) Boldrini, V.; Giovenzana, G. B.; Pagliarin, R.; Pamisano, G.; Sisti, M. *Tetrahedron Lett.* **2000**, *41*, 6527−6530.
(24) Kimura, S.; Bill, E.; Bothe, W.; Weyhermüller, T.; Wieghardt, K. *J. Am. Chem. Soc.* **2001**, *123*, 6025−6039.
(25) Lindsay, J. K.; Hauser, C. R. *J. Org. Chem.* **1957**, *22* (4), 355.
(26) Styka, M. C.; Smierciak, R. C.; Blinn, E. L.; DeSimone, R. E.; Passariello, J. V. *Inorg. Chem.* **1978**, *17*, 82−86.

Table 1. Crystallography Data for **C1**

crystal	**C1**
empirical formula	$C_{19}H_{30}CuFeN_6O_6$
M/g mol^{-1}	557.88
cryst syst	orthorhombic
space group	*Pnma*
a/Å	16.6366(11)
b/Å	9.9935(7)
c/Å	13.6266(9)
V/Å^3	2265.5(3)
Z	4
T/K	123(2)
λ/Å	0.71073
D_c/g cm^{-3}	1.636
μ(Mo Kα)/mm^{-1}	1.628
no. of data measd	12 015
unique data (R_{int})	2602 (0.0322)
obs data [$I > 2(\sigma)I$]	2286
restraints	6
no. of params	208
final R1, wR2 (obs data)	0.0555,[a] 0.1286[b]
final R1, wR2 (all data)	0.0633, 0.1331
ρ_{min}, ρ_{max}/e Å^{-3}	−0.879, 0.926

[a] $R1 = \sum||F_o| - |F_c||/\sum|F_o|$. [b] $wR2 = [\sum w(F_o^2 - F_c^2)^2/\sum w(F_o^2)^2]^{1/2}$.

1307 m, 1240 w, 1124 w, 1081 m, 1035 w, 1012 m, 983 m, 909 w, 868 w, 807 w, 582 w.

X-ray Crystallography. Intensity data for **C1** (0.15 mm × 0.10 mm × 0.08 mm) were measured at 123 K on a Bruker Apex 2 CCD fitted with a graphite-monochromated Mo Kα radiation (0.71073 Å) source. The data were collected to a maximum 2θ value of 55° and processed using the Bruker Apex 2 software. (Collection and refinement parameters are summarized in Table 1.) The structure was solved using Patterson heavy-atom search methods and expanded using standard Fourier routines in the *SHELX97*[28,29] software package. The structure was solved in the space group *Pnma* (attempts to solve it in a lower symmetry space group were unsuccessful, giving an unreasonably high Flack parameter). There was disorder about the cyclen ring with three of the methylene C atoms and the tertiary cyclen N atom located in two distinct positions. These disordered components had their respective site occupancies set to 50%. The coordinating nitrate was also found to be in two discrete positions, each modeled at 50% occupancy. The nitrate N was initially located on the special position (x, 0.75, z), but this gave unreasonable N−O distances. Consequently, it was refined in two positions on either side of the special position and isotropic restrictions were placed on its anisotropic refinement. All H atoms were placed in idealized positions while all non-H atoms were refined anisotropically.

Results and Discussion

Synthesis and Characterization. The ligand 1-(ferrocenemethyl)-1,4,7,10-tetraazacyclododecane (**L**) was obtained via modifications of the synthesis reported by Sisti et al., as described in the Experimental Section.[23] However, a potentially more efficient route to **L** also was attempted in initial experiments. Briefly, following the facile formation of 1,4,7-tris-*tert*-butoxycarbonyl-10-(ferrocenylmethyl)-1,4,7,10-tetraazacyclododecane (**1**) (see Figure 1) by reaction of 1,4,7-tris-*tert*-butoxycarbonyl-1,4,7,10-tetraazacyclododecane[24] with (ferrocenylmethyl)trimethylammonium iodide,[25] it was anticipated that **L** could be obtained by removing the *tert*-butoxycarbonyl protecting groups with trifluoroacetic acid or aqueous solutions of HCl. Unfortunately, this approach was unsuccessful, as ligand **L** could not withstand these cleavage conditions, as previously found by Metzler-Nolte et al. for other ferrocenyl derivatives.[30] Consequently, it was not possible to isolate a stable hydrochloride (or hydrobromide) salt of **L**.

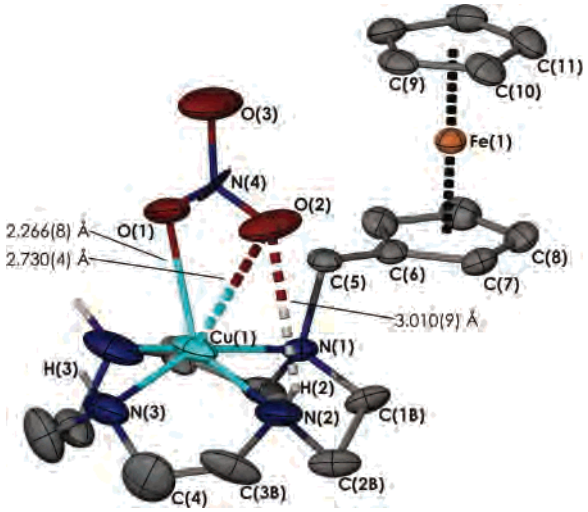

Figure 2. Thermal ellipsoid plot of the complex cation of **C1**. H atoms, a nitrate counterion, and disorder are omitted for clarity (thermal ellipsoids drawn at 50%).

C1 was then obtained by reacting equimolar amounts of $Cu(NO_3)_2 \cdot 3H_2O$ and **L** in ethanol. The complex was precipitated with diethyl ether. IR spectroscopy on **C1** shows characteristic bands at 2918 cm^{-1} corresponding to aromatic C−H stretching. The band at 3179 cm^{-1} could be due to N−H stretching, and the lower than expected frequency could be indicative of hydrogen bonding. The presence of the nitrate groups is confirmed by a strong band at 1382 cm^{-1}. Definitive evidence of the formation of **C1** was obtained by X-ray structural analysis as described below and by the concordance of the microanalysis data with expected values.

X-ray Crystal Structure of C1. The X-ray crystal structure of **C1** (see Figure 2) reveals a highly distorted Cu(II) geometry. Formally, the **C1** coordination sphere is occupied by five bonding atoms, the four N atoms from the cyclen macrocycle and one of the O donors from the nitrate (for bond angles and distances, see Table 2). If we consider the Cu(II) geometry to be distorted square pyramidal, then the basal plane is defined by the N donors, and the Cu(II) resides out of the plane defined by the N_4 ring by 0.513(3) Å, a value similar to that found for the Cu(II) complex of the parent macrocycle, $[Cu(cyclen)(NO_3)]^+$ (**C5**) (see Figure 1).[27] However, the N−Cu−O(1) angles in **C1** vary substantially, viz., 105.0(3)°, 99.3(3)°, 122.9(3)°, 104.2(3)°, and 89.0(4)° for N(1)/N(1)^a/N(2)/N(3)/N(2)^a−Cu(1)−O(1), respectively (symmetry operator a: x, $^3/_2 - y$, z) (see Table

(27) Clay, R.; Murray-Rust, P.; Murray-Rust, J. *Acta Crystallogr., Sect. B: Struct. Crystallogr. Cryst. Chem.* **1979**, *35*, 1894.
(28) Sheldrick, G. M. *SHELXS97*; *Program for Crystal Structure Solution*; University of Göttingen: Göttingen, Germany, 1997.
(29) Sheldrick, G. M. *SHELXL97; Program for Crystal Structure Refinement*; University of Göttingen: Göttingen, Germany, 1997.
(30) Sehnert, J.; Hess, A.; Metzler-Nolte, N. *J. Organomet. Chem.* **2001**, *637*−*639*, 349−355 and references therein.

Table 2. Selected Bond Distances (Å) and Bond Angles (deg) for **C1**[a]

O(1)−Cu(1)	2.266(8)	N(2)−Cu(1)−O(1)	122.9(3)
O(2)−Cu(1)	2.730(4)	N(2)[a]−Cu(1)−O(1)	89.0(4)
Cu(1)−N(1)	2.069(6)	N(3)−Cu(1)−O(1)	104.2(3)
Cu(1)−N(2)	1.999(5)	N(1)[a]−Cu(1)−O(1)	99.3(3)
Cu(1)−N(2)[a]	1.999(5)	N(1)−Cu(1)−O(1)	105.0(3)
Cu(1)−N(3)	2.006(5)	N(2)−Cu(1)−N(2)[a]	148.0(2)
Cu(1)−N(1)[a]	2.069(6)	N(2)−Cu(1)−N(3)	86.63(13)
		N(2)[a]−Cu(1)−N(3)	86.63(13)
		N(2)−Cu(1)−N(1)[a]	95.0(2)
		N(2)[a]−Cu(1)−N(1)	95.0(2)
		N(3)−Cu(1)−N(1)[a]	150.8(2)
		N(3)−Cu(1)−N(1)	150.8(2)

[a] Symmetry operator *a*: $x, {}^3/_2 - y, z$.

Table 3. Hydrogen Bonds for **C1** (Å and deg)

D−H···A	*d*(D−H)	*d*(H···A)	*d*(D···A)	∠(DHA)
N(2)−H(2)···O(2)	0.93	2.64	3.010(9)	100
N(2)−H(2)···O(2)[b]	0.93	1.69	2.607(1)	170
N(2)−H(2)···O(3)[b]	0.93	2.51	3.083(6)	120
N(3)−H(3)···O(4)[a]	0.93	2.23	3.067(6)	150
N(3)−H(3)···O(4)	0.93	2.23	3.067(6)	150

[a] Symmetry operators *a*: $x, {}^3/_2 - y, z$. [b] Symmetry operators *b*: $-x + 1, -y + 2, -z + 1$.

2), whereas in **C5** they were all quite similar (107.8(2)°, 105.9(2)°, 100.6(2)°, and 104.9(2)°). This variation in the N−Cu−O angles in **C1** coupled with the fact that the adjacent N−Cu−N angles vary from 95.0(2)° for N(1)−Cu(1)−N(2)[a] to 86.6(1)° for N(2)−Cu(1)−N(3) (cf. ∼85° in **C5**) leads us to consider the origin of this distortion in the geometry of Cu(1).

Given that in **C5** the nitrate is unidentate and binds perpendicularly to the plane formed by the four cyclen N atoms, the orientation of the second O atom on the nitrate ion toward the Cu^{II} center in **C1** was unexpected. A weak interaction of the second nitrate O with the Cu^{II} center, as well as a hydrogen-bonding interaction between O(2) and the proton on N(2), contribute to this distortion. The Cu(1)−O(1) distance of 2.266(8) Å is typical of apical Cu−O distances for Cu^{II} complexes, which normally exhibit axial elongation. This distance is slightly longer than that found for **C5** (2.183(4) Å).[20] In the case of O(2), the interaction with Cu(1) may be mainly electrostatic rather than coordinative in nature, since the Cu(1)−O(2) distance of 2.730(4) Å is 0.2 Å shorter than the sum of the van der Waals radii of the two atoms (2.92 Å); cf. 0.65 Å for Cu(1)−O(1). The positioning of O(2) may also be affected by a relatively weak hydrogen bond with H(2) reflected by a N···O distance of 3.010(9) Å (see Table 3; H atoms not located). There is a further stronger hydrogen bond between the secondary N atoms on the cyclen rings and the nitrate anions on an adjacent complex (viz., N···O distance of 2.607(1) Å), which may be helping to position the second nitrate O near the Cu^{II} center (Figure 3). A further weaker interaction with the N(3) hydrogen generates a hydrogen-bonded "chelate" ring with the noncoordinating nitrate (N···O 3.067(6) Å).

It is noteworthy that long Cu−O distances have been reported for nitrates chelating to Cu^{II}.[31−33] For example, a

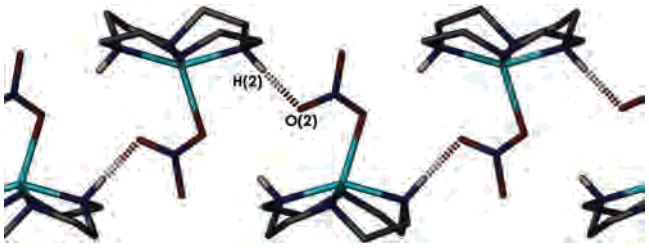

Figure 3. View of hydrogen-bonding interaction connecting adjacent cations in **C1**. The ferrocenyl moiety is omitted for clarity.

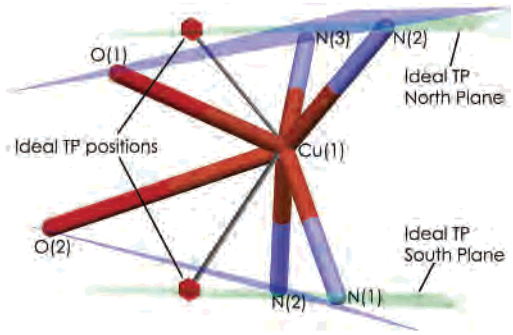

Figure 4. Stick representation plot of the Cu coordination sphere, highlighting the pseudo-trigonal-prismatic (TP) geometry (blue planes show planes north and south of the prism; red hexagons represent the O positions of ideal TP geometry).

Cu−O distance of 2.568(3) Å was reported by Wisniewski et al.[34] for bis(2-(4′-thiazolyl)benzimidazole-*N*,*N*′)nitratocopper(II) nitrate and of 2.674(1) Å by Casellas et al. for a trinuclear Cu^{II} complex.[35] Reedijk and co-workers reported an analysis of the structure of a series of complexes of tripodal tetradentate ligands (Cu^{II}, Ni^{II}, and Cd^{II}) in which they proposed three bonding modes for nitrate anions: monodentate for Cu^{II} [difference in two Cu−O distances >0.6 Å); anisodentate (asymmetric) for Cd^{II} (difference in two Cd−O distances 0.3−0.6 Å); and bidentate for Ni^{II} (difference in two Ni−O distances <0.3 Å)].[36] Applying this analysis, the difference in Cu−O distances in **C1** (0.46 Å) suggests anisodentate coordination of nitrate. Regardless of the nature of the interaction between O(2) and the Cu^{II} center in **C1** (i.e., whether this is an electrostatic interaction or weak coordination) and whether this arises because of electrostatic, hydrogen bonding, and/or crystal-packing effects, it is clear that the orientation of the nitrate imposes severe geometric distortion on the metal center.

Examination of the organization of the donor atoms and the Cu^{II} center indicates that the Cu^{II} geometry may be described as trigonal prismatic (see Figure 4). This type of geometry is quite commonly observed for metal sulfides,

(31) Bernarducci, E. E.; Bharadwaj, P. K.; Lalancette, R. A.; Krogh-Jespersen, K.; Potenza, J. A.; Schugar, H. J. *Inorg. Chem.* **1983**, *22*, 3911−3920.

(32) Prasad, B. L. V.; Sato, H.; Enoki, T.; Cohen, S.; Radhakrishnan, T. P. *J. Chem. Soc., Dalton Trans.* **1999**, 25−29.

(33) Marjani, K.; Davies, S. C.; Durrant, M. C.; Hughes, D. L.; Khodemorad, N.; Samodi, A. *Acta Crystallogr., Sect. E: Struct. Rep. Online* **2005**, *E16*, m11−m14 and references therein.

(34) Wisniewski, M. Z.; Glowiak, T.; Opolski, A.; Wietrzyk, J. *Met.-Based Drugs* **2001**, *8*, 189.

(35) Casellas, H.; Gamez, P.; Reedijk, J.; Mutikainen, I.; Turpeinen, U.; Maschiocchi, N.; Galli, S.; Sironi, A. *Inorg. Chem.* **2005**, *44*, 7918.

(36) Kleywegt, G. J.; Wiesmeijer, W. G. R.; Van Driel, G. J.; Driessen, W. L.; Reedijk, J.; Noordik, J. H. *J. Chem. Soc., Dalton Trans.* **1985**, 2177−2184.

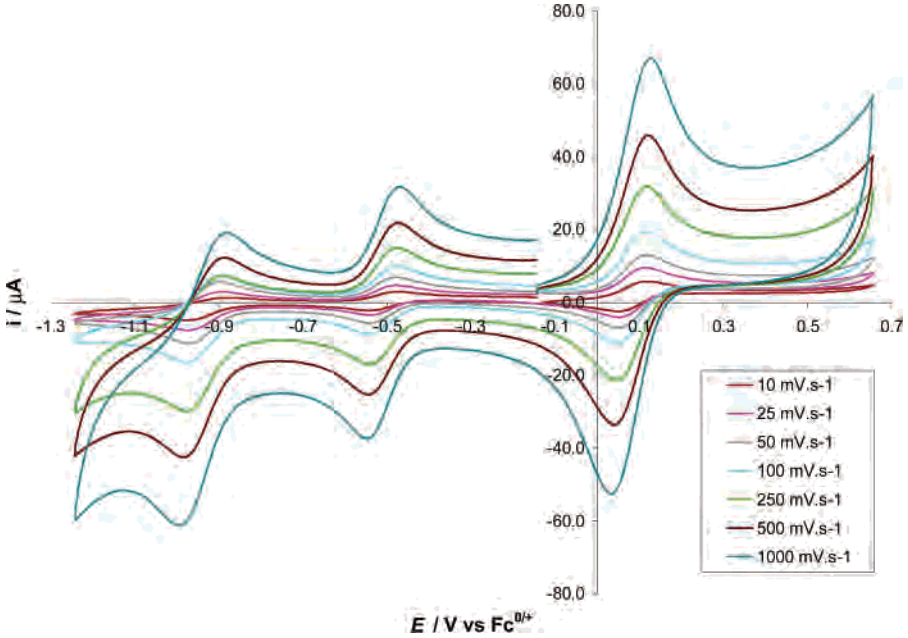

Figure 5. Cyclic voltammograms at 20 °C of **C1** (1 mM) at a GC electrode, in acetonitrile with $[Bu_4N][NO_3]$ (0.1 M) as the supporting electrolyte. Experiments were undertaken over a scan-rate range of 10−1000 mV s^{-1} and with Cp^*_2Fe as the internal reference (0.25 mM). Potentials are referenced to the $Fc^{0/+}$ scale using Cp^*_2Fe as a secondary standard (−505 mV vs $Fc^{0/+}$).

such as MoS_2 and WS_2,[37] but it is also found in a number of complexes of first-row transition-metal complexes (see, for example, publications which report catechol macrobicyclic metal complexes[38] and the structures of $[Mn(acac)_2bpy]$[39] and manganese(II)(picolinydenehydrazyl)(2-pyridyl)methane[40]). The trigonal prism is collapsed with the north and south faces bending toward each other (see Figure 4). This is highlighted by the intersection angle of the least-squares planes defined by O(2), N(1), and N(2) and O(1), N(3), and N(2)^a (symmetry operator a: x, $^3/_2 - y$, z) as 23.6(4)°.

Electrochemical Studies. Voltammetric investigations of complex **C1** were carried out at a stationary GC electrode in acetonitrile to ascertain if binding of the nitrate anion to the Cu^{II} center was retained in the solution phase. Tetrabutylammonium nitrate ($[Bu_4N][NO_3]$) was used as the supporting electrolyte (0.1 M) in initial experiments to facilitate retention of coordinated nitrate when the complex is dissolved in this potentially coordinating solvent. Decamethylferrocene (Cp^*_2Fe) was used as a secondary reference compound for the potential scale calibration, instead of the usual Fc, to avoid overlap with the Fc(**C1**) oxidation process. The potential of the $Cp^*_2Fe^{0/+}$ process is close to −500 mV vs $Fc^{0/+}$ in most solvents,[41] and potentials have been converted to the $Fc^{0/+}$ scale (see Experimental Section for details). Cyclic voltammograms of **C1** over the scan rate range of 10−1000 mV s^{-1} are presented in Figure 5. The process centered close to −500 mV vs $Fc^{0/+}$ corresponds to the $Cp^*_2Fe^{0/+}$ secondary reference, the one in the 100 mV region vs $Fc^{0/+}$ corresponds to the $Fc^{0/+}$(**C1**) couple, and the one at about −900 mV vs $Fc^{0/+}$ corresponds to the $Cu^{II/I}$**(C1)** couple. The $Fc^{0/+}$(**C1**) and Cu**(C1)**$^{II/I}$ processes have the same characteristics in the absence of Cp^*_2Fe.

Both the **C1** oxidation and reduction reactions exhibit separations in their peak potentials and scan-rate dependence similar to those found for the known reversible one-electron $Cp^*_2Fe^{0/+}$ process. Thus, complex **C1** is concluded to exhibit a reversible one-electron oxidation process with a formal potential $E°_f$ of +85 mV vs $Fc^{0/+}$ and a reversible one-electron reduction couple with an $E°_f$ value of −932 mV vs $Fc^{0/+}$, as determined from the average of the oxidation and reduction peak potentials (value given applies at a scan rate of 100 mV s^{-1} but is almost independent of the scan rate). The reactions associated with the redox couples are assigned in their simplest forms, as in eqs 1 and 2

$$Fc^0(\mathbf{C1}) \rightarrow Fc^+(\mathbf{C1}) + e^- \quad (1)$$

$$Cu^{II}(\mathbf{C1}) + e^- \rightarrow Cu^{I}(\mathbf{C1}) \quad (2)$$

Previous electrochemical studies of Cu^{II}−cyclen derivatives have found that the voltammograms for the $Cu^{I/II}$ process were not reproducible. This has been attributed to a rearrangement of the reduced complex brought about by the inability of the cyclen cavity to bind and stabilize the +I oxidation state for copper.[42] Hence, the observed reversibility and almost ideal voltammetry of the $Cu^{II/I}$ process in our case is deserving of comment. The Cu^{I}−cyclen complex

(37) Cotton, F. A.; Wilkinson, G.; Murillo, C. A.; Bochmann, M. *Advanced Inorganic Chemistry*, 6th ed.; Wiley: Chichester, U.K., 1999.
(38) Karpishin, T. B.; Stack, T. D. P.; Raymond, K. N. *J. Am. Chem. Soc.* **1993**, *115*, 182−192.
(39) van Gorkum, R.; Buda, F.; Kooijman, H.; Spek, A. L.; Bouwman, E.; Reedijk, J. *Eur. J. Inorg. Chem.* **2005**, 2255−2261.
(40) Gupta Sreerama, S.; Pal, S.; Pal, S. *Inorg. Chem. Commun.* **2001**, *4*, 656−660.
(41) Noviandri, I.; Brown, K. N.; Fleming, D. S.; Gulyas, P. T.; Lay, P. A.; Masters, A. F.; Phillips, L. *J. Phys. Chem. B* **1999**, *103*, 6713−6722.
(42) El Ghachtouli, S.; Cadiou, C.; Déchamps-Olivier, I.; Chuburu, F.; Aplincourt, M.; Turcry, V.; Le Baccon, M.; Handel, H. *Eur. J. Inorg. Chem.* **2005**, 2658−2668 and references therein.

Scheme 1. Schematic Representation of Possible Equilibria Established in Acetonitrile and Their Influence on the Reduction and Oxidation of **C1**−**C4**

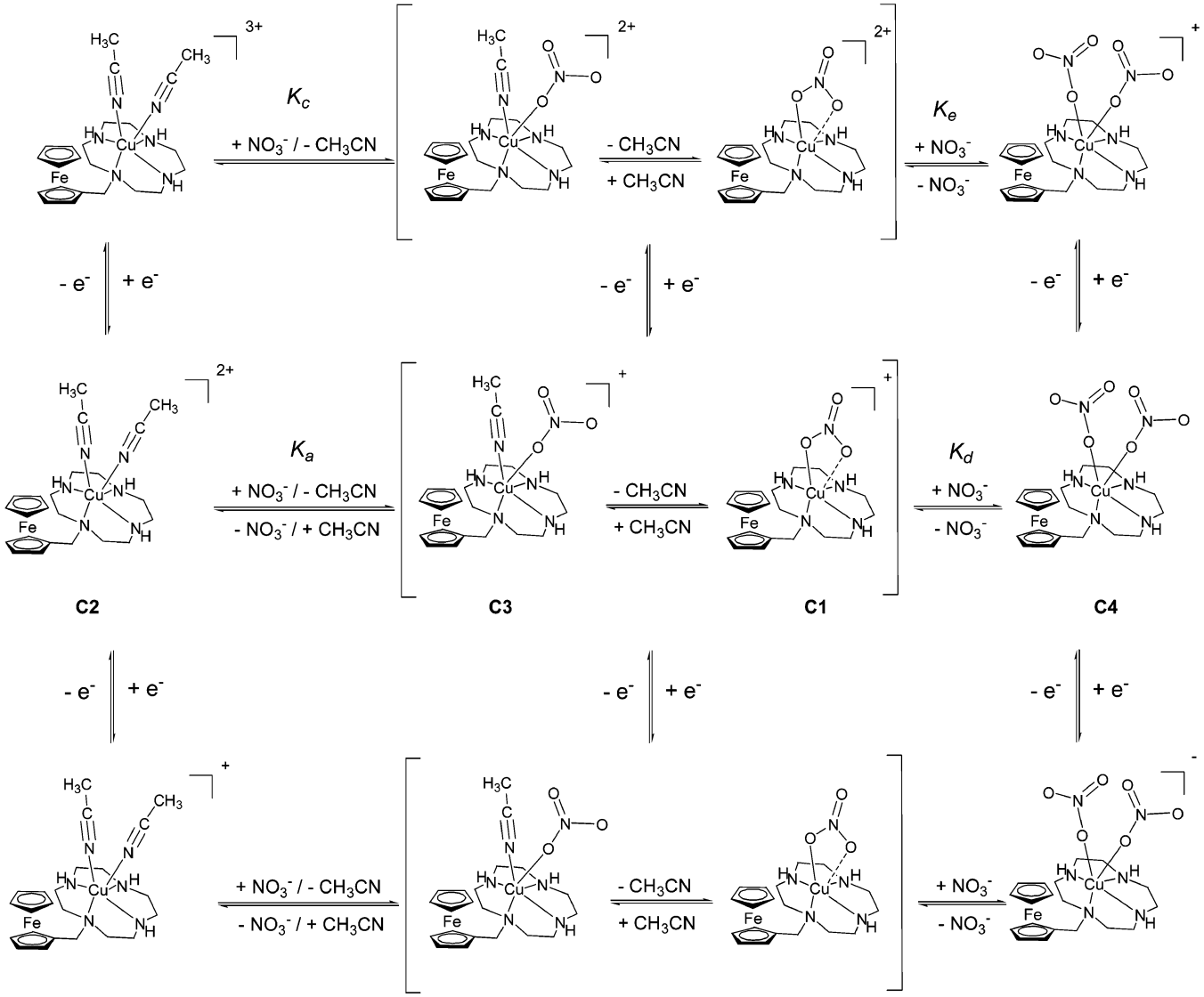

formed following reduction will prefer to adopt a tetrahedral geometry or one of lower coordination number, although it would be expected that this rearrangement will be countered by the structural constraints of the cyclen macrocycle. However, the propensity for acetonitrile to bind strongly to and stabilize the Cu^I state means that it is possible that the nitrate ion(s) will be substituted by acetonitrile molecule(s) upon reduction of **C1**. It is also feasible that nitrate(s) may be released on reduction without binding of acetonitrile, but in this case the Cu^I coordination sphere would be occupied by the four macrocycle N atoms and the constrained macrocyclic structure would make it difficult for the Cu^I center to adopt its preferred tetrahedral geometry. An alternative possibility is that upon reduction one or more of the macrocycle N donors become substituted by acetonitrile ligands. In each of these scenarios, the reduction to Cu^I and oxidation back to the Cu^{II} state will be accompanied by significant structural changes. The fact that the $Cu^{II/I}$ process is reversible under these circumstances indicates that the chemical processes associated with these structural changes are fast on the electrochemical time scale.

When the supporting electrolyte was changed to tetrabutylammonium hexafluorophosphate ($[Bu_4N][PF_6]$), significant shifts in $E°_f$ values to more positive potentials were detected for both processes (Supporting Information, Figure S1). In the presence of 0.1 M $[Bu_4N][PF_6]$, the $E°_f$ value for the $Cu^{II/I}$**(C1)** process was −825 mV vs $Fc^{0/+}$ and +128 mV vs $Fc^{0/+}$ for the $Fc^{0/+}$(**C1**) process. Thus, the absence of the NO_3^- ion in the supporting electrolyte makes reduction easier and oxidation more difficult. This electrolyte−anion dependence implies the presence of rapid equilibria between complexes **C1**, **C2**, **C3**, and **C4**, as in Scheme 1. On the basis of the UV−vis measurements (see below), the species present in solution (in the Cu^{II} state) are assumed to be hexacoordinated in the range of nitrate concentrations studied. The presence of analogous equilibria in oxidized and reduced forms is also suggested in Scheme 1.

When $[Bu_4N][PF_6]$ is used as the electrolyte, it is assumed that PF_6^- is an innocent noncoordinating ligand as, to the best of our knowledge, no structures of Cu^{II}−cyclen derivatives with a coordinated PF_6^- anion have been reported. Although there are also no reports of Cu^{II}−cyclen derivatives

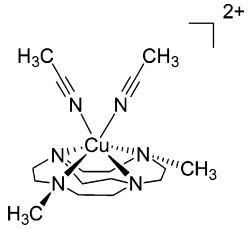

Figure 6. Structure of Cu^{II} complex with two acetonitrile ligands reported by Hubin et al.[43]

with one acetonitrile molecule bound to the Cu^{II} center and only one example of a hexacoordinated Cu^{II}−cyclen derivative complex with two acetonitrile molecules,[43] structures of Cu^{II} complexes of tetraazamacrocycles bearing one acetonitrile molecule[44−51] or two acetonitrile molecules or nitrile derivatives[52−57] are available. In the case of the hexacoordinated Cu^{II}−cyclen derivatives, the ligand was a strapped cyclen macrocycle (two trans N atoms of the macrocycle are linked via an ethylene bridge; see Figure 6). This has a significant effect on the way that the macrocycle binds to Cu^{II}. The complex adopts a distorted octahedral geometry with a cis configuration of the monodentate acetonitriles as observed for octahedral Ni^{II} complexes of cyclen derivatives with two water molecules.[58,59] In our case, the more flexible macrocyclic structure would be expected to encourage the formation of a square-pyramidal coordination geometry (as observed previously for other systems and [Cu(cyclen)(NO$_3$)]$^+$) (**C5**; see Figure 1).[60] Only minor distortion to this coordination polyhedron is required to allow NO_3^- binding as found in **C1**. Nevertheless, the UV−vis measurements (see below) suggest that the complexes present in solution are not pentacoordinate square pyramidal or even trigonal pyramidal. This leads to the conclusion that the structure of **C2** in solution is hexacoordinate as depicted in Figure 1 and similar to the one reported in the solid state by Hubin et al.[43]

To further investigate the electrochemical behavior of **C1**, a voltammetric study was performed with different ratios of [Bu$_4$N][PF$_6$] and [Bu$_4$N][NO$_3$] as the supporting electrolyte (at constant ionic strength of 0.1 M). Cyclic voltammograms are displayed in Figure 7, and reversible potential data are shown in Figure 8. A gradual shift to more positive potentials was observed for both Fc$^{0/+}$(**C1**) and Cu$^{II/I}$(**C1**) redox centers when the concentration of [Bu$_4$N][PF$_6$] was increased. This supports the hypothesis that as the nitrate concentration is lowered, acetonitrile preferentially binds the Cu^{II} center, which makes the Fc^0(**C1**) complex harder to oxidize and the Cu^{II}(**C1**) complex easier to reduce due to the replacement of a negatively charge moiety (nitrate ion) by the solvent ligand. Acetonitrile is also likely to bind even more strongly to Cu^I than Cu^{II} (see Scheme 1). Consequently, a larger shift is observed for the Cu$^{II/I}$(**C1**) center (+107 mV) compared with the Fc$^{0/+}$(**C1**) (+39 mV) center when the electrolyte is changed from 0.1 M [Bu$_4$N][NO$_3$] to 0.1 M [Bu$_4$N][PF$_6$].

If solvent coordination is neglected and it is assumed that the system involves only a change in the number of coordinated nitrate anions as in eq 3

$$[\text{Fc}-\text{Cu cyclen}-(\text{NO}_3^-)_p]^{n+} + (n-m)\text{e}^- \rightleftharpoons [\text{Fc}-\text{Cu cyclen}-(\text{NO}_3^-)_q]^{m+} + (p-q)\text{NO}_3^- \quad (3)$$

then the relationship given in eq 4 would be expected to apply when the nitrate concentration is high.[61]

$$E^\circ_{\text{f,obs}} = E^\circ_{\text{f}} + \frac{RT}{2(n-m)F}\ln\frac{D_{\text{red}}}{D_{\text{ox}}} - \frac{RT}{(n-m)F}\ln\frac{K_{\text{ox}}}{K_{\text{red}}} - (p-q)\frac{RT}{(n-m)F}\ln[\text{NO}_3^-]_{\text{tot}} \quad (4)$$

Abbreviations used in eq 3 are as follows: $E^\circ_{\text{f,obs}}$ = formal potential in the presence of nitrate; E°_{f} = formal potential in the absence of nitrate; R = gas constant; T = temperature; F = Faraday constant; D = diffusion coefficient; K = equilibrium constant; $n - m$ = number of electron(s) exchanged in the electron-transfer process (=1 in our case); $p - q$ = difference in the number of nitrates bound to Cu in the two oxidation states; $[NO_3^-]_{tot}$ = total concentration of nitrate in solution; ox and red are subscripts used to report the oxidized and reduced [Fc−Cu cyclen−$(NO_3^-)_p$]$^{n+}$ and [Fc−Cu cyclen−$(NO_3^-)_q$]$^{m+}$ complexes, respectively.

In the present case, $n - m = 1$ and D_{ox} and D_{red} can be assumed to be equal. The curvature in the plot in Figure 8 is therefore consistent with more than one oxidized and reduced species being present over the nitrate concentration range examined. The limiting slope of about 40 mV in the E versus ln[NO$_3$]$_{tot}$ plot at high nitrate concentration in Figure 8, calculated assuming eq 4 applies, would imply that $p - q$ approaches 2. If $p - q$ were 2, the result could be

(43) Hubin, T. J.; Alcock, N. W.; Morton, M. D.; Busch, D. H. *Inorg. Chim. Acta* **2003**, *348*, 33.
(44) Comba, P.; Juristic, P.; Lampeka, Y. D.; Peters, A.; Prikhod'ko, A. I.; Pritzkow, H. *Inorg. Chim. Acta* **2001**, *324*, 99.
(45) Bucher, C.; Moutet, J.-C.; Pecaut, J.; Royal, G.; Saint-Aman, E.; Thomas, F. *Inorg. Chem.* **2004**, *43*, 3777.
(46) Bernhardt, P. V.; Moore, E. G.; Riley, M. J. *Inorg. Chem.* **2001**, *40*, 5799.
(47) Di Casa, M.; Fabbrizzi, L.; Licchelli, M.; Poggi, A.; Sacchi, D.; Zema, M. *J. Chem. Soc., Dalton Trans.* **2001**, 1671.
(48) Herrera, A. M.; Staples, R. J.; Kryatov, S. V.; Nazarenko, A. Y.; Rybak-Akimova, E. V. *Dalton Trans.* **2003**, 846.
(49) Brooker, S.; Hay, S. J.; Plieger, P. *Angew. Chem., Int. Ed.* **2000**, *39*, 1968.
(50) Brooker, S.; Kelly, R. J.; Moubaraki, B.; Murray, K. S. *Chem. Commun.* **1996**, 2579.
(51) Warzeska, S.; Kramer, R. *Chem. Commun.* **1996**, 499.
(52) Kim, J. C.; Fettinger, J. C.; Kim, Y. I. *Inorg. Chim. Acta* **1999**, *286*, 67.
(53) Scott, M. J.; Holm, R. H. *J. Am. Chem. Soc.* **1994**, *116*, 11357.
(54) Ballester, L.; Gutierrez, A.; Perpinan, M. F.; Sanchez, A. E.; Azcondo, M. T.; Gonzalez, M. J. *Inorg. Chim. Acta* **2004**, *357*, 1054.
(55) Oshio, H. *Inorg. Chem.* **1993**, *32*, 4123.
(56) Ellis, L. T.; Perkins, D. F.; Turner, P.; Hambley, T. W. *Dalton Trans.* **2003**, 2728.
(57) Ballester, L.; Gil, A. M.; Gutierrez, A.; Perpinan, M. F.; Azcondo, M. T.; Sanchez, A. E.; Amador, U.; Campo, J.; Palacio, F. *Inorg. Chem.* **1997**, *36*, 5291.
(58) Lai, C.-Y.; Lan, W.-J.; Wang, C.; Chung, C.-S. *Polyhedron* **1998**, *17*, 2127−2136.
(59) Bencini, A.; Bianchi, A.; Garcia-Espana, E.; Jeannin, Y.; Julve, M.; Marcelino, V.; Philoche-Levisalles, M. *Inorg. Chem.* **1990**, 29, 963−970.
(60) Styka, M. C.; Smierciak, R. C.; Blinn, E. L.; DeSimone, R. E.; Passariello, J. V. *Inorg. Chem.* **1978**, *17*, 82−86.
(61) Heyrovsky, J.; Kuta, J. *Principles of Polarography*; Academic Press: New York, 1966; p 156.

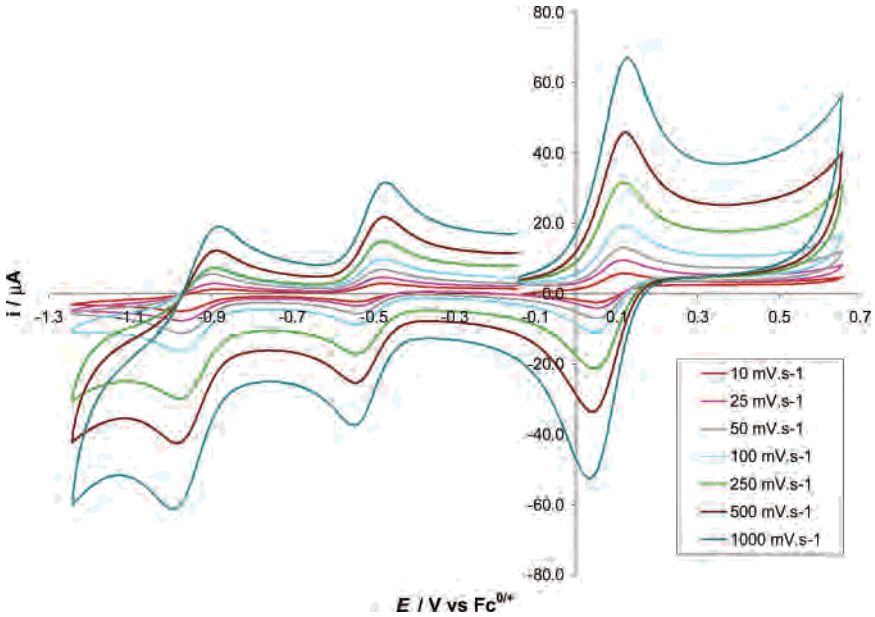

Figure 7. Cyclic voltammograms of **C1** (1 mM) at a GC electrode, in acetonitrile with different ratios of supporting electrolyte $[Bu_4N][PF_6]$ and $[Bu_4N][NO_3]$ (the total electrolyte concentration was maintained constant at 0.1 M). All experiments were undertaken at a scan rate of 100 mV s^{-1} and at 20 °C with Cp^*_2Fe as the internal reference (0.25 mM). Potentials are referenced to $Fc^{0/+}$ with Cp^*_2Fe as the secondary standard (−505 mV vs $Fc^{0/+}$).

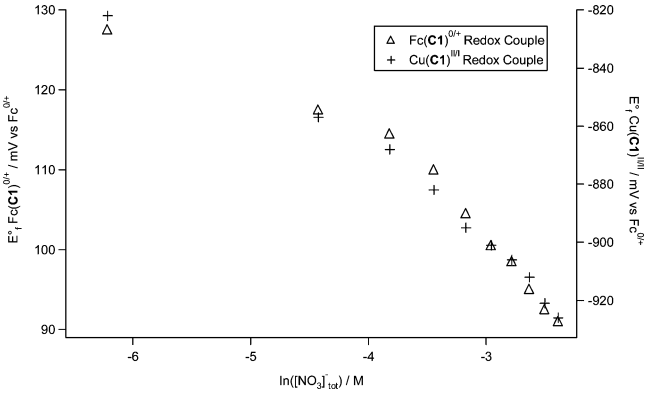

Figure 8. Variation of $E°_f$ for the $Cu^{II/I}$(**C1**) and $Fc^{0/+}$(**C1**) redox centers as a function of ln(concentration of $[Bu_4N][NO_3]$) (electrolyte concentration maintained at 0.1 M with $[Bu_4N][PF_6]$).

interpreted in terms of reduction of the Cu^{II} center containing two coordinated nitrates to a Cu^{I} containing no coordinated nitrate.[61] However, this limiting scenario is clearly not achieved, and the process is assumed to involve a range of species as in Scheme 1, where acetonitrile coordination needs to be considered and the solvent only replaces or partially replaces the nitrate ligand upon reduction of the Cu^{II} center to the Cu^{I} state. Extended equations apply for these more complex scenarios as summarized in Scheme 1. To establish the full set of equilibria that describe this system, detailed knowledge of the species present in all redox levels is required. Such information is not presently available, albeit spectrophotometric data (see below) provide additional information concerning the nature of the Cu^{II} species present.

A brief study of the electrochemical behavior of the copper^{II}−cyclen complex, nitrato(1,4,7,10-tetraazacyclododecane)copper^{II} nitrate (**C5**) (See Figure 1), was undertaken to compare the affinity of this complex for the nitrate anion. **C5** was synthesized following the procedure described by Styka et al.[26] Clay and co-workers subsequently reported the X-ray structure of **C5** in which the binding of the nitrate anion to the copper center was found to be perpendicular to the plane of the cyclen macrocycle and through only one oxygen atom.[27]

Cyclic voltammograms of **C5** over the scan rate range of 10−1000 mV s^{-1} with $[Bu_4N][NO_3]$ as the supporting electrolyte are presented in Figure 9 (cyclic voltammograms obtained with 0.1 M $[Bu_4N][PF_6]$ as the supporting electrolyte are presented in Supporting Information, Figure S2). In this case, the redox reaction centered at about −500 mV corresponds to the $Cp^*_2Fe^{0/+}$ process and the one at −1000 mV vs $Fc^{0/+}$ corresponds to the $Cu^{I/II}$(**C1**) process.

With 0.1 M $[Bu_4N][NO_3]$ as the supporting electrolyte and for fast scan rates, complex **C5** exhibits a reversible one-electron reduction process with an $E°_f$ value of −993 mV vs $Fc^{0/+}$, as determined from the average of the oxidation and reduction peak potentials (value given at a scan rate of 250 mV s^{-1}). The process in the fast-scan regime is assigned to the reversible $Cu^{II/I}$ reduction of complex **C5** containing coordinated nitrate. However, as seen by the inspection of Figure 9, the process exhibits chemical irreversibility when the scan rate is ≤250 mV s^{-1}. In contrast, the behavior was fully reversible at all scan rates examined when the supporting electrolyte was 0.1 M $[Bu_4N][PF_6]$. Interestingly, the shift in the formal potential for the $Cu^{II/I}$ redox processes of **C1** and **C5** upon replacement of $[Bu_4N][NO_3]$ by $[Bu_4N][PF_6]$ as the supporting electrolyte is similar (Table 4). This suggests that the presence of the Fc pendant group does not have a major influence on the equilibrium constants for nitrate complexation in acetonitrile media.

To further analyze the role of the solvent and the importance of the binding of nitrate, electrochemical measurements on **C1** were carried out in nitromethane solution. Nitromethane is likely to be a poorly coordinating solvent that will bind only weakly to both Cu^{I} and Cu^{II}. Under these

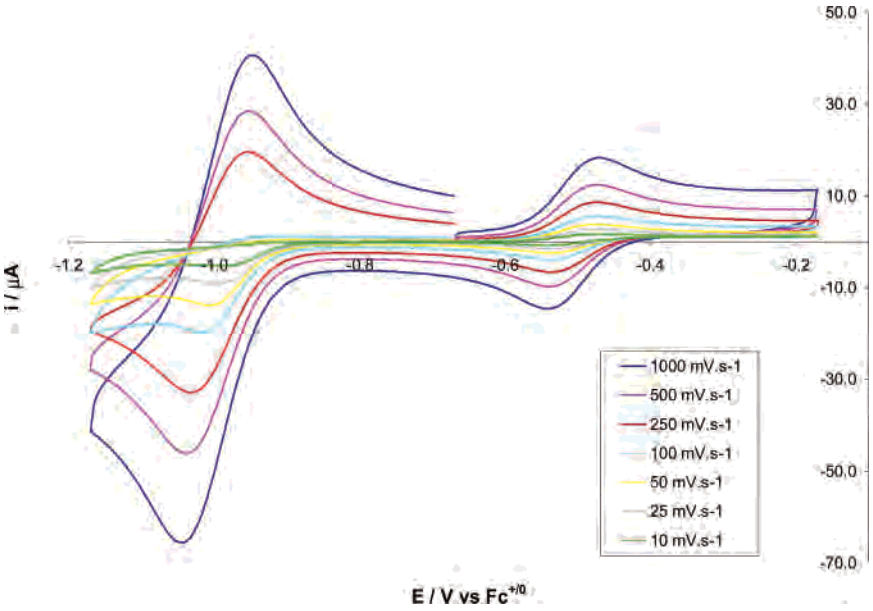

Figure 9. Cyclic voltammograms of **C5** (1 mM) at a GC electrode, in acetonitrile with $[Bu_4N][NO_3]$ (0.1 M) as the supporting electrolyte. Experiments were undertaken over the scan-rate range of 10−1000 mV s^{-1} at 20 °C with Cp^*_2Fe as the internal reference (0.25 mM). Potentials are referenced to $Fc^{0/+}$ with Cp^*_2Fe as the secondary standard (−505 mV vs $Fc^{0/+}$).

Table 4. Formal Potentials for the $Cu^{II/I}$(**C1**) and $Cu^{II/I}$(**C5**) Processes in Acetonitrile with 0.1 M $[Bu_4N][NO_3]$, 0.1 M $[Bu_4N][PF_6]$, or a 0.05 M Mixture of These Supporting Electrolytes (Ionic Strength = 0.1 M)[d]

redox couple	$E°_f$[a]/mV (0.1 M $[Bu_4N][NO_3]$)	$E°_f$[a]/mV (0.05 M $[Bu_4N][NO_3]$ and 0.05 M $[Bu_4N][PF_6]$)	$E°_f$[a]/mV (0.1 M $[Bu_4N][PF_6]$)	$\Delta E°_{fmax}$/mV
$Cu^{II/I}$(**C1**)	−932[b]	−901[b]	−824[b]	108[b]
$Cu^{II/I}$(**C5**)	−993[c]	−964[c]	−884[c]	109[c]

[a] vs $Fc^{0/+}$. [b] Value reported at a scan rate of 100 mV s^{-1}. [c] Value reported at a scan rate of 250 mV s^{-1}. [d] $\Delta E°_{fmax} = E°_f$ with 0.1 M $[Bu_4N][PF_6]$ electrolyte − $E°_f$ with 0.1 M $[Bu_4N][NO_3]$ electrolyte.

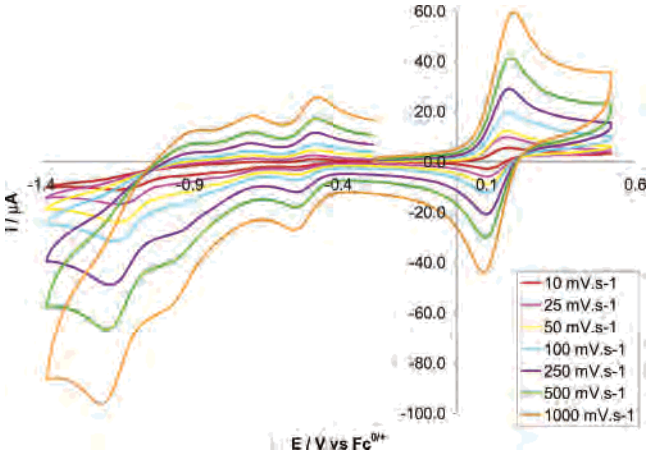

Figure 10. Cyclic voltammograms of **C1** (1 mM) at a GC electrode, in nitromethane with Bu_4NPF_6 (0.1 M) as the supporting electrolyte. Experiments were undertaken over the scan-rate range of 10−1000 mV s^{-1} at 20 °C with Cp^*_2Fe as the internal reference (0.25 mM). Potentials are referenced to $Fc/Fc^{0/+}$ with Cp^*_2Fe as the secondary standard (−508 mV vs $Fc^{0/+}$).

circumstances, the nitrate binding for **C1** should be significantly stronger than that found in acetonitrile and hence the Cu^{II} center would be expected to be more difficult to reduce. Cyclic voltammograms of **C1** in nitromethane with 0.1 M $[Bu_4N][PF_6]$ as the supporting electrolyte are presented in Figure 10. The wave centered at about −500 mV corresponds to the $Cp^*_2Fe^{0/+}$ process, and the one at about +150 mV (vs $Fc^{0/+}$) corresponds to the $Fc^{0/+}$(**C1**) process. However, the $Cu^{II/I}$ reduction is now far more complex than in acetonitrile, and at least three reduction processes instead of a single process are observed at negative potentials vs $Cp^*_2Fe^{0/+}$.

Complex **C1** exhibits a reversible one-electron oxidation process in nitromethane. The process is assigned to the reversible $Fc^{0/+}$ oxidation and has a formal potential $E°_f$ of +136 mV vs $Fc^{0/+}$, as determined from the average of the oxidation and reduction peak potentials (value given at a scan rate of 100 mV s^{-1} but almost independent of the scan rate). Importantly, the $E°_f$ value is similar to that found for **C1** in acetonitrile with noncoordinating $[Bu_4N][PF_6]$ (0.1 M) as the supporting electrolyte (+128 mV vs $Fc^{0/+}$). In contrast, the fact that at least three processes are detected for the $Cu^{II/I}$ redox couple with 0.1 M $[Bu_4N][PF_6]$ as the electrolyte is a strong indication of the thermodynamic (and kinetic) importance of the binding of solvent in acetonitrile. The voltammetric reduction of **C1** in nitromethane is assumed to involve a mixture of poorly solvated nitrate complexes being transformed to an extremely weakly or even nonsolvated Cu^{I} center upon reduction, whereas in acetonitrile strongly solvated forms are dominant unless $[Bu_4N][NO_3]$ is present as an electrolyte.

When sufficient $[Bu_4N][NO_3]$ was present in the supporting electrolyte in nitromethane (at a constant ionic strength of 0.1 M), the cyclic voltammograms became significantly

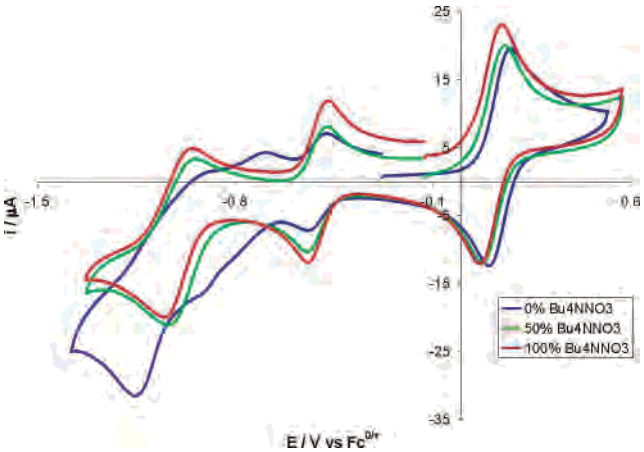

Figure 11. Cyclic voltammograms of **C1** (1 mM) at a GC electrode, in nitromethane with different ratios of supporting electrolyte $[Bu_4N][PF_6]$ and $[Bu_4N][NO_3]$ (the total electrolyte concentration was always kept at 0.1 M). Experiments were undertaken at a scan rate of 100 mV s^{-1} and at 20 °C with Cp^*_2Fe as the internal reference (0.25 mM). Potentials are referenced to $Fc^{0/+}$ with Cp^*_2Fe as the secondary standard (−508 mV vs $Fc^{0/+}$).

simplified (Figure 11). Instead of three processes in the absence of $[Bu_4N][NO_3]$, only a single essentially reversible process was now observed for the $Cu^{II/I}$ redox couple. Furthermore, the $E°_f$ values observed when either 50% (0.05 M) or 100% (0.1 M) nitrate was present in the nitromethane solution were almost constant, with only minor shifts of −4 and −7 mV for the $Fc^{0/+}$(**C1**) and $Cu^{II/I}$(**C1**) redox couples, respectively, being detected over the nitrate concentration range. In acetonitrile solution, on the other hand, shifts of −10 and −35 mV for the $Fc^{0/+}$(**C1**) and $Cu^{II/I}$(**C1**) cases, respectively, accompanied the same change in nitrate concentration. This result provides clear evidence that solvent coordination is considerably more significant in acetonitrile than in nitromethane and that nitrate may remain coordinated to the Cu^I center when nitromethane is used as the solvent.

UV−Vis Spectrophotometric Studies. To provide further insight into the Cu^{II} species present in acetonitrile solutions of **C1**, UV−vis spectral measurements were undertaken (Figure 12) at varying nitrate concentrations (different ratios of $[Bu_4N][PF_6]$ and $[Bu_4N][NO_3]$ so that a 1:1 mixture of **L** and $Cu(ClO_4)_2·6H_2O$ (0.5 mM) in 0.1 M $[Bu_4N][PF_6]$ in acetonitrile (top graph in Figure 12) at a constant ionic strength of 0.1 M and at $T = 298$ (±0.2) K was achieved).

The spectra exhibit two main features: a band at ∼440 nm, which corresponds to a Fe^{II} d−d transition of the Fc moiety, and a second more intense band at ∼600 nm due to a Cu^{II} d−d transition. Interestingly, no bands were observed between 900 and 1500 nm for all the spectra measured, which is a feature of square-pyramidal Cu^{II} complexes.[62−64] This indicates that the Cu^{II} complexes present in solution are not pentacoordinate square pyramidal,[62−64] and the spectra are typical for an octahedral Cu^{II} complex. Although a square-planar geometry is also consistent with the observed spectrum, the variation in the spectra with added nitrate mitigates against this possibility. Importantly, a significant spectral change is observed even when small amounts of nitrate are added to the acetonitrile solution, viz., shifts of +10 nm for the d−d transition of Cu^{II} due to the introduction of O donors in place of a N donor and −7 nm for the d−d transition of Fc when only 2.5% of $[Bu_4N][NO_3]$ is added to the solution that contains 0% of $[Bu_4N][NO_3]$. Corresponding values for the 100% nitrate solutions are ca. +20 nm for the d−d transition of Cu^{II} and ca. −25 nm for the d−d transition of Fc. Moreover, the spectrum of the complex prepared in situ in the absence of nitrate (1:1 mixture of **L** and $Cu(ClO_4)_2·6H_2O$ in an acetonitrile solution containing 0.1 M $[Bu_4N][PF_6]$) is different from that of **C1** dissolved in acetonitrile, which would contain 2 mol equiv of nitrate.

As the above experiments involving the in situ generated complex introduced water into the solutions (from the copper salt), the spectra were recorded following the addition of known amounts of water to solutions of the in situ prepared complex and **C1** to assess whether the interpretation of the spectrophotometric (and electrochemical data) could be complicated by the presence of small amounts of water. Our findings were as follows: (i) No change in the spectrum was observed when small aliquots of water (up to 10 mM) were deliberately added to the in situ generated 1:1 complex. (ii) No change in the spectrum was observed when small aliquots of water (≤10 mM) were added to an acetonitrile solution of 0.5 mM **C1** (0.1 M $[Bu_4N][PF_6]$). (iii) Minor spectral changes were observed when the measurements were carried out in water (0.5 mM **C1**) without added electrolyte (for solubility reasons). We also note that similar minor spectral changes were observed when the spectrum of **C5** was measured in water (cf., methanol) and in the solid state.[60] On the basis of these results, it is reasonable to assume that under the conditions used (≤10 mM water) acetonitrile coordination is dominant over water coordination and, in keeping with this conclusion, only the equilibria involving acetonitrile coordination to Cu^{II} need to be considered, as in Scheme 1. Hence, the initial change in the spectra in Figure 12 is probably due to the replacement of coordinated acetonitrile by nitrate ions, which indicates that the value of the equilibrium constant for the binding of the first nitrate (K_a in Scheme 1) is large. Further addition of nitrate therefore results in coordination of a second nitrate ion. The presence of the dinitrate complex **C4** in solution corroborates with the voltammetric finding that $p - q$ approaches 2 (see above). Thus, the electronic spectra support the conclusion revealed on the basis of the electrochemical data that at least two Cu^{II}−nitrate complexes exist in acetonitrile.

The apparent molar extinction coefficient, ϵ_{APP}, determined at 593 nm in acetonitrile decreases systematically as the concentration of nitrate increases (Figure 13). With the assumption that one nitrate is already bound to the Cu^{II} ion,

(62) Hathaway, B. J. In *Comprehensive Coordination Chemistry*; Wilkinson, G., Gillard, R. D., McCleverthy, J. A., Eds.; Pergamon Press: Oxford, England, 1987; Vol. 5, p 533.
(63) McLachlan, G. A.; Fallon, G. D.; Martin, R. L.; Spiccia, L. *Inorg. Chem.* **1995**, *34* (1), 254−261.
(64) Brudenell, S. J.; Spiccia, L.; Bond, A. M.; Comba, P.; Hockless, D. C. R. *Inorg. Chem.* **1998**, *37* (15), 3705−3713.

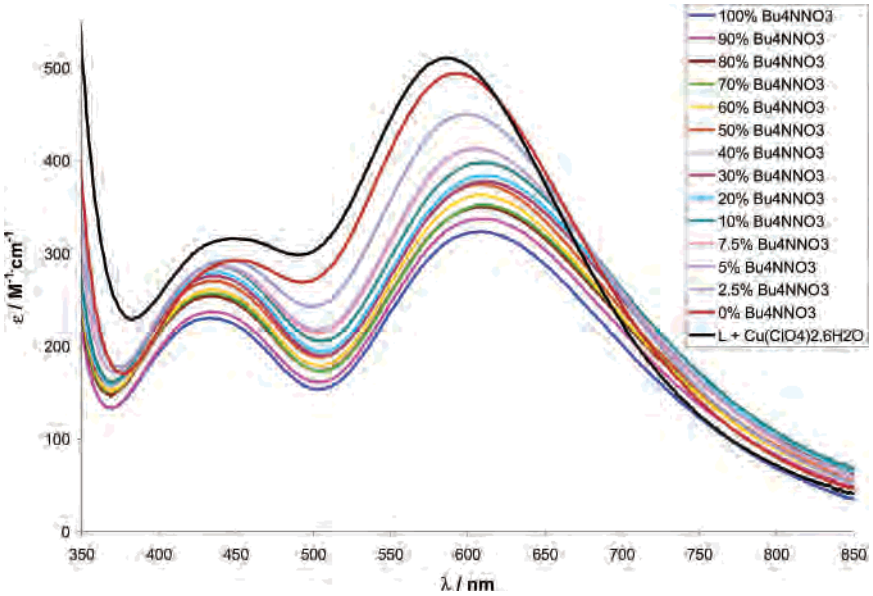

Figure 12. UV−vis spectra of **C1** (0.5 mM) measured in acetonitrile for solutions containing different ratios of $[Bu_4N][PF_6]$ and $[Bu_4N][NO_3]$ and a 1:1 mixture of **L** and $Cu(ClO_4)_2{\cdot}6H_2O$ in 0.1 M $[Bu_4N][PF_6]$ in acetonitrile (I = 0.1 M; T = 298 K).

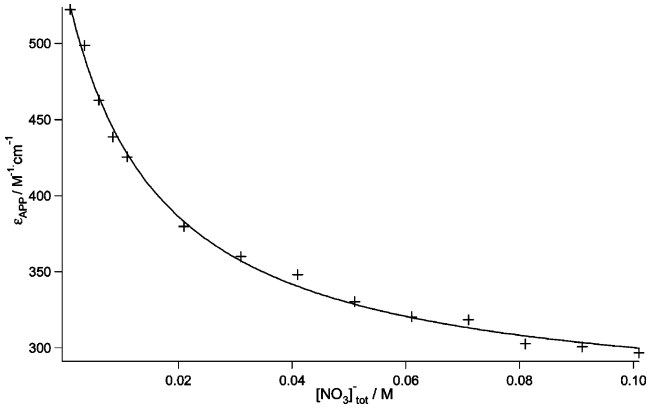

Figure 13. Dependence of ϵ_{APP} at 593 nm as a function of $[NO_3]^-$ ($C_{\mathbf{C1}}$ = 0.5 mM; I = 0.1 M; T = 298 K) as determined experimentally (+) and with the calculated fit (line) based on $\epsilon_{\mathbf{C1}} = 540 \pm 5$ M^{-1} cm^{-1}, $\epsilon_{\mathbf{C4}} = 261 \pm 5$ M^{-1} cm^{-1}, and $K_d = 61 \pm 5$ M^{-1}.

as suggested by all spectral data, this can be interpreted in terms of a single nitrate concentration-dependent equilibrium, e.g.

$$\mathbf{C1}\ (\text{or}\ \mathbf{C3}) + NO_3^- \rightleftharpoons \mathbf{C4}\ \text{or}\ \{\mathbf{C1} + \mathbf{C3}\} + NO_3^- \rightleftharpoons \mathbf{C4} \quad (5)$$

The spectral data were analyzed using eq 6, which was derived on the basis that two complexes exist in equilibrium ($\mathbf{C1} + NO_3^- \rightleftharpoons \mathbf{C4}$).

$$\epsilon_{APP} = \frac{A}{[Cu^{2+}]_{tot}} = \frac{\epsilon_{\mathbf{C1}} + \epsilon_{\mathbf{C4}} K_d [NO_3^-]_{tot}}{1 + K_d [NO_3^-]_{tot}} \quad (6)$$

(where A = absorbance; $\epsilon_{\mathbf{C1}}$ = extinction molar coefficient of **C1**; $\epsilon_{\mathbf{C4}}$ = extinction molar coefficient of **C4**; $K_d = [\mathbf{C4}]/([[NO_3^-][\mathbf{C1}])$ = equilibrium constant). An analogous equation would apply if **C1** and **C3** were present in equilibrium. The analysis of data under these circumstances would lead to the same value of K_{app}, but the value of $\epsilon_{\mathbf{C1}}$ would represent a composite value derived from **C1** and **C3**.

An excellent fit to the data was obtained (see the solid line in Figure 13) using the following parameters: $\epsilon_{\mathbf{C1}} = 540 \pm 5$ M^{-1} cm^{-1}, $\epsilon_{\mathbf{C4}} = 261 \pm 5$ M^{-1} cm^{-1}, and $K_d = 61 \pm 5$ M^{-1}. Analysis of the data to determine the binding constant of the first nitrate was not possible, but an estimate of 1000 M^{-1} can be made from the change in absorbance at low $[NO_3]^-$.

UV−vis measurements also were carried out in nitromethane. In this case, the spectra of **C1** at 0 and 0.1 M concentrations of added nitrate are nearly identical (see Supporting Information). As in acetonitrile, no bands were observed between 900 and 1500 nm. This suggests that the geometry of the Cu^{II} centers of the species present in a nitromethane solution is also octahedral and that the dominant species present in a nitromethane solution should be **C4**, even when no nitrate had been added.

To determine if the "special" binding of the nitrate observed in the solid state for **C1** was present in solution, UV−vis measurements were carried out on a solution of **C5**, a compound that does not exhibit this type of binding in the solid state (see above). The results (see Supporting Information) were similar to those found for **C1**, and no bands were observed between 900 and 1500 nm for **C5**. The square-pyramidal geometry for **C5** appears to be present only in the solid state. This adds further support to the equilibria proposed for compounds **C1**−**C4** in Scheme 1.

In summary, both UV−vis and electrochemical studies imply that in nitrate-containing acetonitrile solutions, complexes **C1** (and/or **C3**) and **C4** are the major species in equilibrium. In the weakly coordinating solvent nitromethane, unlike the case in acetonitrile, the extent of nitrate complexation remains significant even in neat solvent due to the lack of solvent competition.

Conclusions. An unusual solid-state Cu^{II} geometry has been identified for the Cu^{II}−nitrate complex of a cyclen

derivative ligand bearing a ferrocenyl unit, when compared with the complex without the ferrocenyl pendant. The Cu^{II} center is surrounded by four N atoms of the macrocycle and two O atoms of a nitrate anion, one of which exhibits a typical form of coordination while the other interacts more weakly. The nature of the binding of the nitrate anion in the solution phase also has been investigated by electrochemical and UV−vis spectrophotometric measurements. In acetonitrile, substantial changes in redox potential are obtained for the $Fc^{0/+}$ and $Cu^{II/I}$ redox couples (+39 and +107 mV for the $Fc^{0/+}$(**C1**) and $Cu^{I/II}$(**C1**) redox couples, respectively) when 0.1 M $[Bu_4N][PF_6]$ is used instead of 0.1 M $[Bu_4N][NO_3]$ as the electrolyte, suggesting that solvated forms of Cu^{II} and Cu^{I} are important in this medium. **C5** also exhibits analogous behavior in acetonitrile in terms of the nitrate binding ability. UV−vis spectral measurements on the Cu^{II} form of **C1** indicate that the equilibrium constant for binding of the first nitrate is $\sim$1000 M^{-1}, whereas the value for the second nitrate is 61 $\pm$ 5 M^{-1}. Thus, the nitrate anion also has a high affinity for the Cu^{II} center in this system when dissolved in acetonitrile. Voltammetric studies in the less-coordinating solvent nitromethane containing 0.1 M $[Bu_4N][PF_6]$ as the electrolyte imply that nitrate complexation is significant even in neat solvent. Different electrochemical behavior for the $Cu^{II/I}$ redox couple, relative to that found in acetonitrile, is associated with weaker solvent coordination. In contrast, the voltammetry of the $Fc^{0/+}$ redox couple is not strongly solvent-dependent.

Acknowledgment. This work was supported by the Swiss National Science Foundation and the Australian Research Council (ARC) through the Australian Centre for Electromaterials Science (ACES) and an Australian Postgraduate Award to M.J.B. G.G. was the recipient of a Swiss Fellowship for Prospective Researchers Grant (PBNE2-106771). The authors thank Ms. Zuzanna Kosowski for the technical assistance provided during a vacation scholarship.

Supporting Information Available: Cyclic voltammograms of **C1** (1 mM) in acetonitrile with $[Bu_4N][PF_6]$ (0.1 M) as the supporting electrolyte (Figure S1), cyclic voltammograms of **C5** (1 mM) in acetonitrile with $[Bu_4N][PF_6]$ (0.1 M) as the supporting electrolyte (Figure S2), UV−vis spectra of **C1** (0.5 mM) measured in nitromethane for solutions containing different ratios of $[Bu_4N][PF_6]$ and $[Bu_4N][NO_3]$ (Figure S3), UV−vis spectra of **C5** (0.5 mM) measured in nitromethane for solutions containing different ratios of $[Bu_4N][PF_6]$ and $[Bu_4N][NO_3]$ (Figure S4), and crystallographic data for **C1** in CIF format. This material is available free of charge via the Internet at http://pubs.acs.org.

IC061622+